Supporting Information

All-Perfluorosulfonated-Ionomer Composite Membranes Containing Blow-Spun Fibers: Effect of a Thin Fiber Framework on Proton Conductivity and Mechanical Properties

Shuta Onuki,[†, ¶] Yoshiki Kawai,[†,*, ¶] Hiroyasu Masunaga,[‡] Noboru Ohta,[‡] Ryohei Kikuchi,[§] Minoru Ashizawa,[†] Yuta Nabae[†], and Hidetoshi Matsumoto[†,*]

[†] Department of Materials Science and Engineering, Tokyo Institute of Technology, 2-12-1 Ookayama, Meguro-ku, Tokyo 152-8552, Japan

[‡] Japan Synchrotron Radiation Research Institute, 1-1-1 Kouto, Sayo, Hyogo 679-5198, Japan

[§] Materials Analysis Division, Open Facility Center, Tokyo Institute of Technology, 2-12-1 Ookayama, Meguro-ku, Tokyo 152-8550, Japan

*Address correspondence to matsumoto.h.ac@m.titech.ac.jp and kawai.y.ag@m.titech.ac.jp

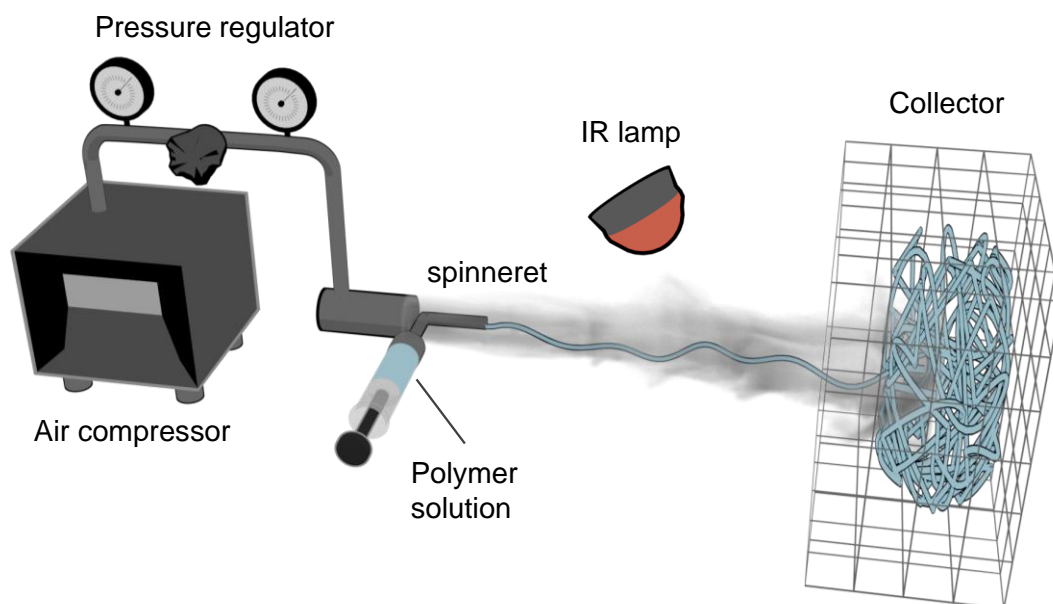[¶] Shuta Onuki and Yoshiki Kawai contributed equally.

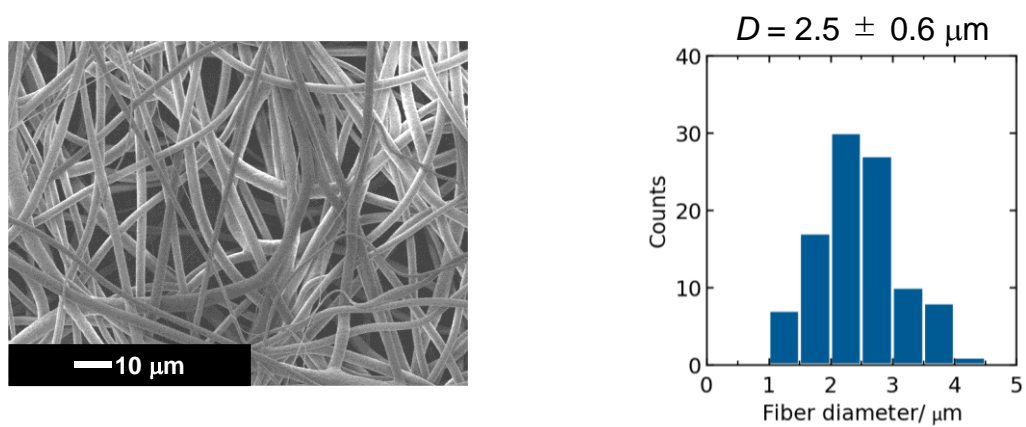**Figure S1.** Schematic of the apparatus used for blow spinning.

Figure S2. Surface SEM image and the fiber diameter distributions, determined by SEM image analysis, for the hot-pressed PVDF thin-fiber webs.
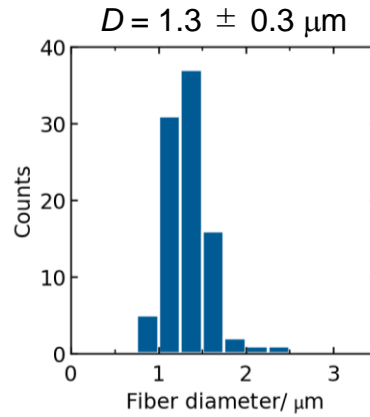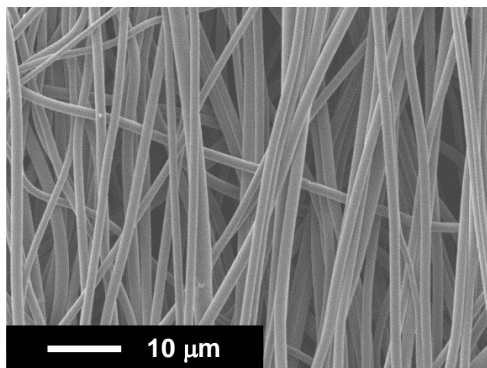
Figure S3. Surface SEM image and the fiber diameter distributions, determined by SEM image analysis, for the as-spun aligned PFSA thin-fiber sheets with a second-order parameter S of 0.86. The alignment of the thin fibers in the sheets was determined from the SEM images using a second-order parameter calculated using the ImageJ software. The second-order parameter S was defined according to the following equation [1]:

$$S = 2(cos^2\theta) - 1 = cos2\theta \qquad (1)$$

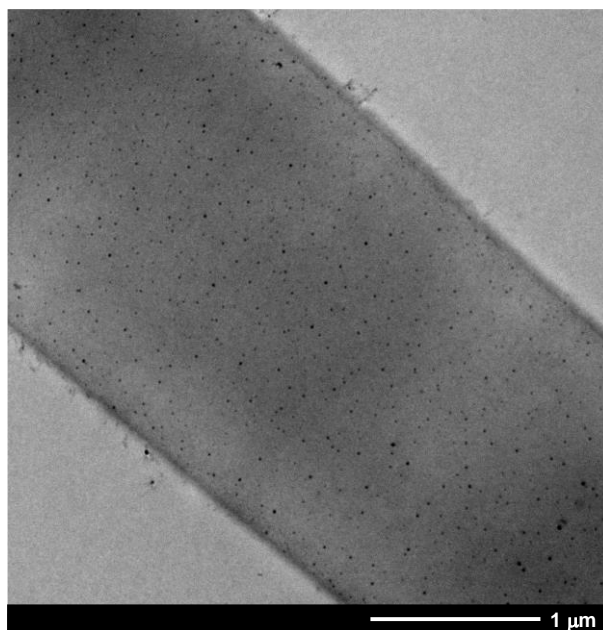where θ is the angle between the direction of the fibers and vertical direction in the SEM image.

Figure S4. Typical TEM image of the post-treated PFSA thin fiber. The counterions of the PFSA thin fiber were exchanged with Ag$^+$.
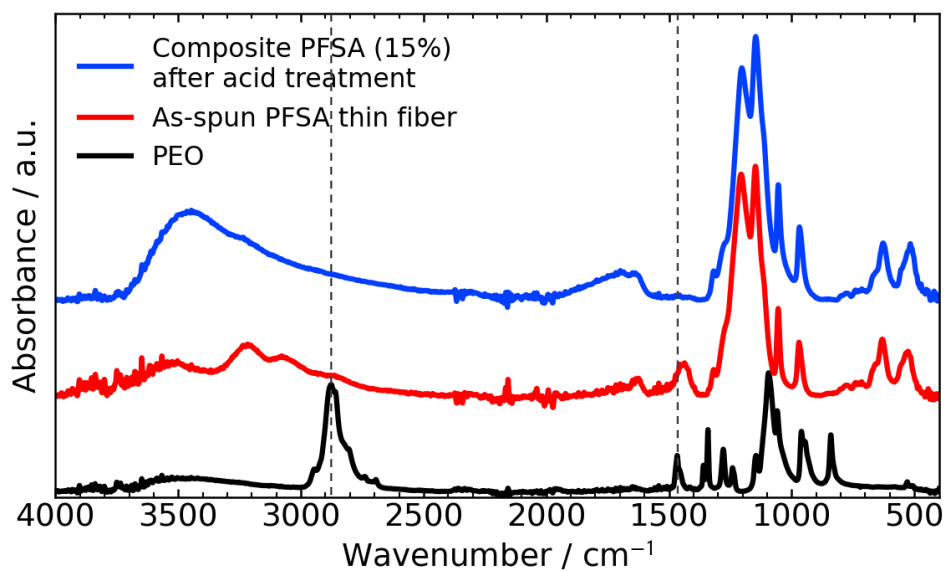

Figure S5. FTIR spectra of the all-PFSA thin-fiber composite PEMs (thin fiber content of 15 wt%) after acid treatment.
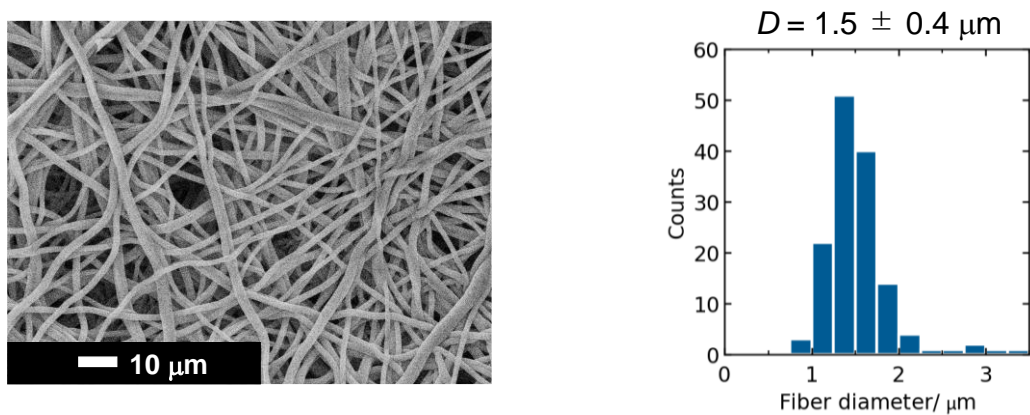
Figure S6. Surface SEM image and the fiber diameter distribution, determined by SEM image analysis, for the hot-treated PFSA thin-fiber webs after acid treatment.

Figure S7. Typical stress–strain curves of the pristine and composite PFSA membranes.

Figure S8. Temperature dependence of the proton conductivity through the PVDF thin-fiber composite (15 wt%) and PFSA thin-fiber composite (15 wt%) membranes at 90 %RH.
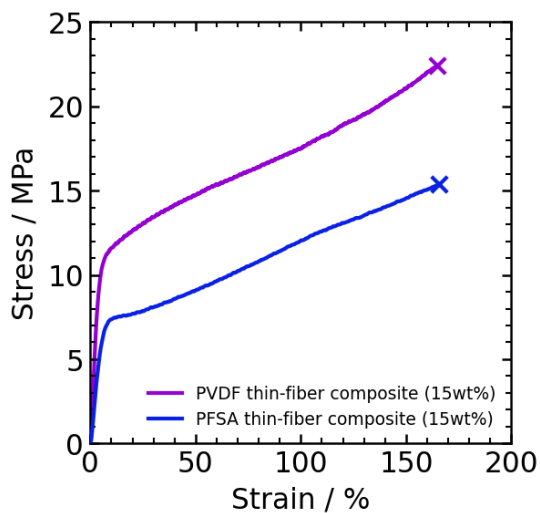
Figure S9. Stress–strain curve of the PVDF thin-fiber composite (15 wt%) and PFSA thin-fiber composite (15 wt%) membranes.

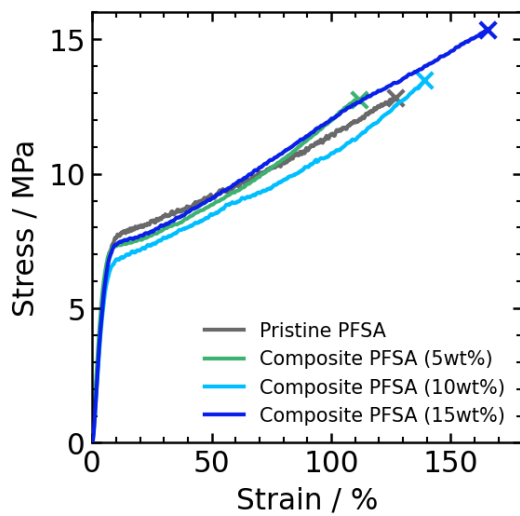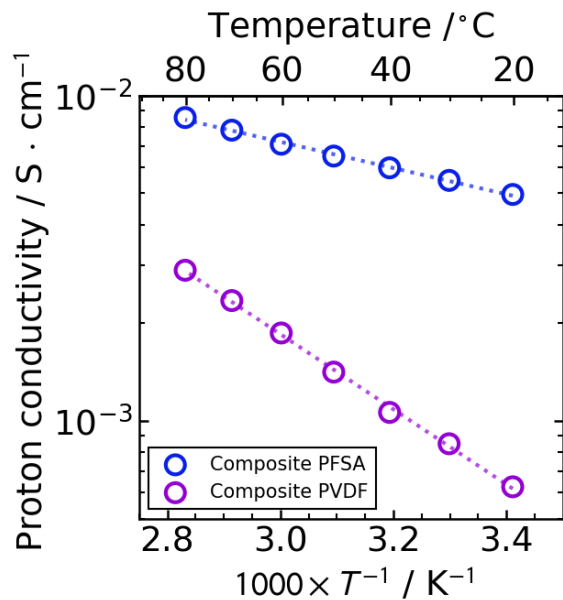**Figure S10** shows typical TGA and DSC curves of the pristine and composite PFSA membranes. Both membranes exhibited a similar thermal behavior. For the TG curves, the gradual weight loss of approximately 6-8 % in the range from 25 to 180 °C would be due to the loss of water molecules. The sharp weight loss at approximately at 280 °C would be associated with desulfonation [2]. For the DSC curves, an endothermic peak near 113 °C attributed to the glass transition behavior of amorphous ionic domains of PFSA was observed [2].

Figure S10. Typical (a) TGA and (b) DSC curves of the pristine and composite PFSA membranes (thin fiber content of 15 wt%).

Table S1. Reported FC performances of representative PEMs

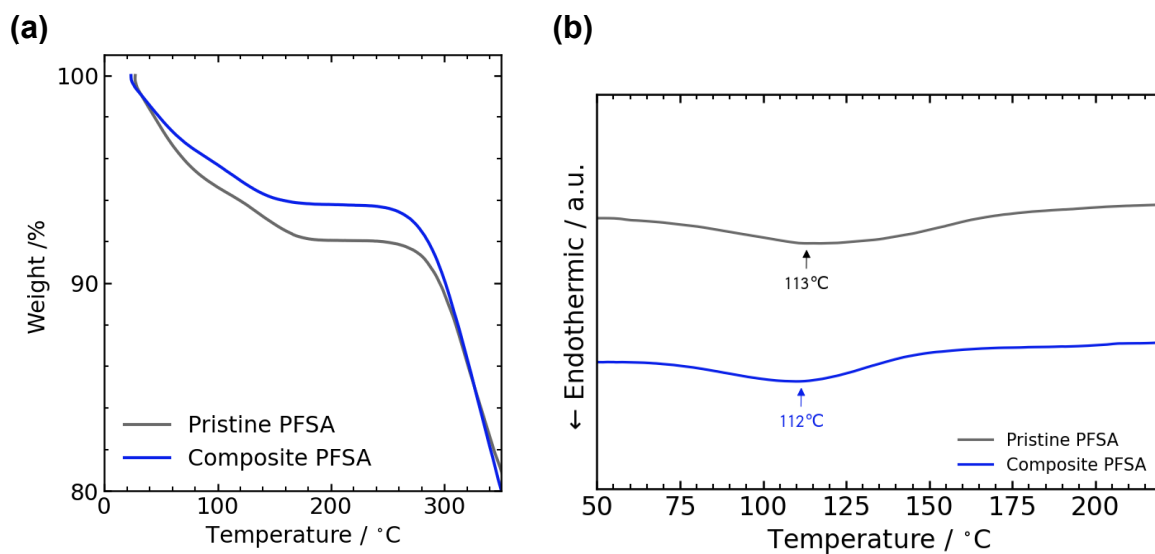| PEM	Thickness [um]	Temperature [°C]	RH [%]	P_{max} [mW cm^{-2}]	Conditions	Reference
Composite PFSA (15 wt%)	**39**	**80**	**100**	**1,324 @0.05 V**	MEA area: 1cm^2, 0.4 mg-Pt cm^{-2}, H$_2$/O$_2$ without back pressure	**This Work**
	36	**120**	**25**	**300 @0.35 V**		
PhySPI: PBI(8:2)BNF /Nafion	5	80	100	680*	@ 0.4V 25cm^2, 0.4 mg-Pt cm^{-2}, H$_2$/O$_2$ without back pressure	[3]
		120	24	176		
Nafion NR-211	25	80	100	520*		
		120	24	112		
Nafion polymer	20	80	95	1,469 @2.6 A cm^{-2}	25cm^2, 0.4 mg-Pt cm^{-2}, H$_2$/air with backpressure 150 kPa and 140 kPa for anode and cathode, respectively.	[4]
		110	25	153 @0.9 A cm^{-2}		
SCC PFSA	20	80	95	1,588 @2.6 A cm^{-2}		
		110	25	279 @0.9 A cm^{-2}		
Nafion-212	51	110	25	121	5 cm^2, 0.5 mg-Pt cm^{-2}, H$_2$/O$_2$ without back pressure	[5]
sPSU-SGO	50–55	110	25	183		
sPSU	50–55	110	25	38		
3M 660/PPSU-NF Composite membrane	51	80	93	630*	@0.6 V 5 cm^2, 0.25 mg-Pt cm^{-2} (prior to fuel cell testing, MEAs were briefly soaked in 1M H$_2$SO$_4$), H$_2$/air without back pressure	[6]
		120	25	144*		
Nafion NR-211	25	80	93	479*		
		120	25	60*		
PVDFHFP/Nafion -DMD	12	80	95	1570	4 cm^2, 0.5 mg-Pt cm^{-2}, H$_2$/O$_2$ without back pressure	[7]
		120	35	450		
Nafion HP	20	80	95	1330		

		120	35	420		
PEI/Aquivion-SiO$_2$/HPA	30–50	120	40	660	No information of MEA area, 0.4 mg-Pt cm^{-2}, H$_2$/O$_2$ without back pressure	[8]
Aquivion E87-05S	50	120	40	410		
Aquivion E79-03S (Solvicore 6 cells compressed at 15 kg cm^{-2})	30	80	100	727 @ 0.72 V	360 cm^2, 0.6–0.8 mg-Pt cm^{-2}, H$_2$/air at 1.5 bar.	[9]
		110	33	401 @ 0.5V		
Aquivion E79-03S (Solvicore 6 cells compressed at 13 kg cm^{-2})		80	100	600 @0.6 V		
		120	25	237 @0.59 V		
Aquivion E79-03S (JMFC 5 cells compressed at 10 kg cm^{-2})		80	100	675		
		110	33	370		
Aquivion E79-03S (Solvicore 5 cells compressed at 10 kg cm^{-2})		80	100	730		
		120	25	261		

*Calculated data from Reference.

Abbreviations: PFSA, perfluorosulfonic acid; Phy, phytic acid; SPI, sulfonated polyimide; PBI, polybenzimidazole; BNF, blend polymer nanofibers; SSC, short-side-chain; sPSU, sulfonated polysulfone; SGO, organo-sulfonated derivative of the graphene oxide; 3M 660, Perfluorosulfonic acid with EW of 660 from 3M Company; PPSU-NF, polyphenylsulfone nanofiber; PVDF-HFP, poly(vinylidene fluoride-*co*-hexafluoropropylene; DMD, direct membrane deposition; PEI, poly(ether imide); SiO$_2$/HPA, SiO$_2$/heteropolyacid nanoparticles; JMFC, Johnson Matthey fuel cells.
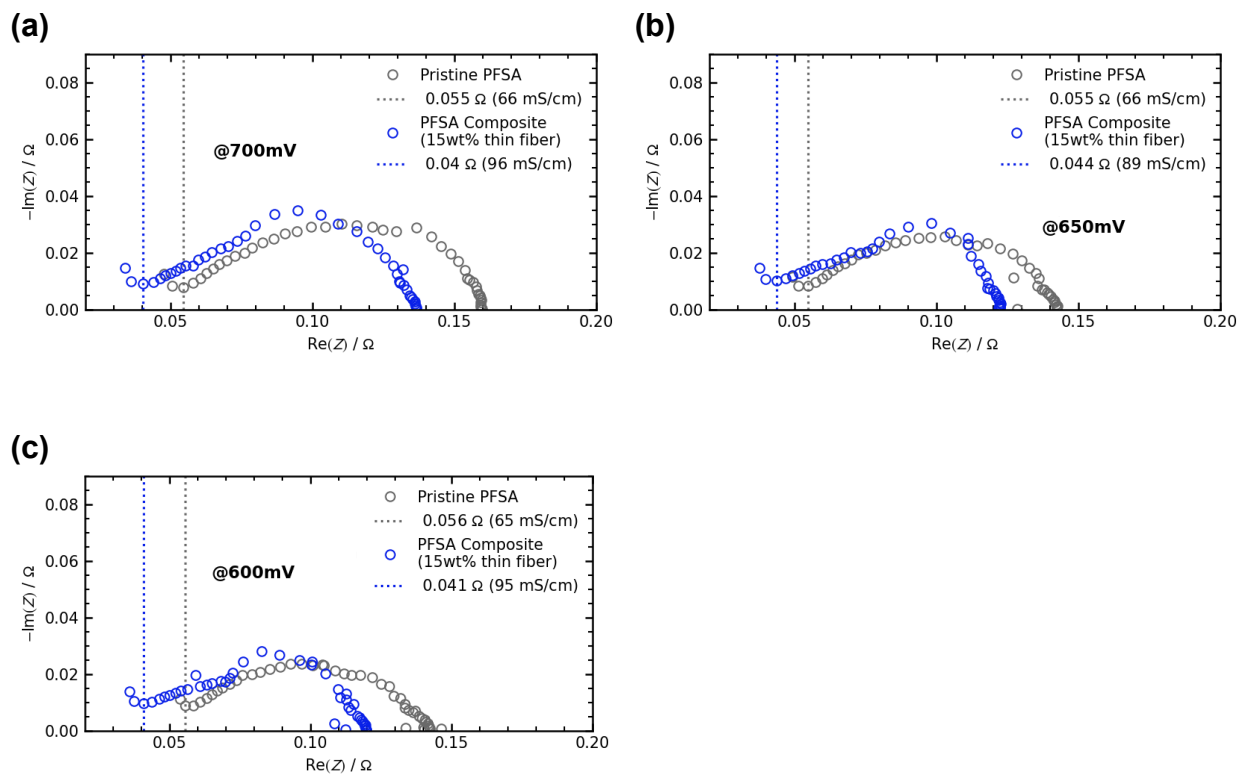
(a)

(b)

(c)

Figure S11. Nyquist plots of the FCs operated in (a) 0.7 V, (b) 0.65 V, and (c) 0.6 V at 80°C

(100% RH@anode and 81% RH@cathode). The dotted lines show R_{ohm}.

Figure S12. Nyquist plots of the FCs operated in (a) 0.7 V, (b) 0.65 V, and (c) 0.6 V at 100°C (47% RH@anode and 38% RH@cathode). The dotted lines show R_{ohm}.
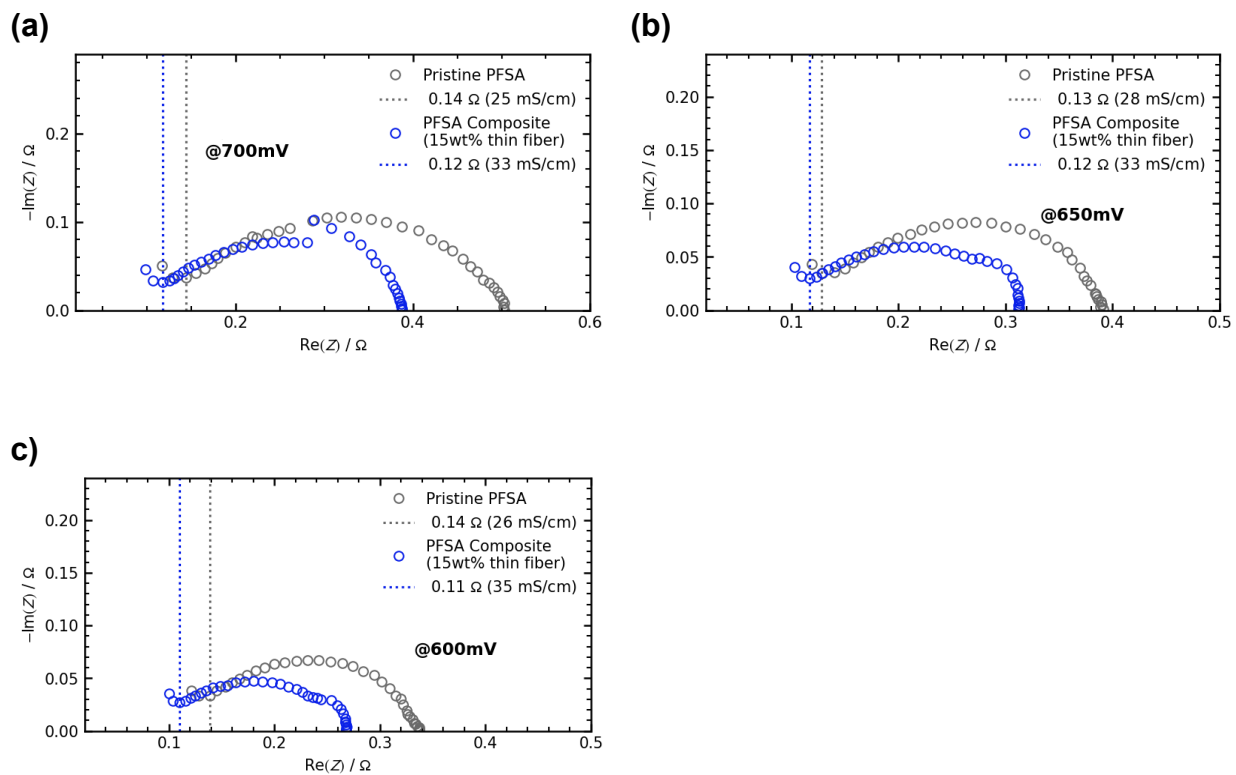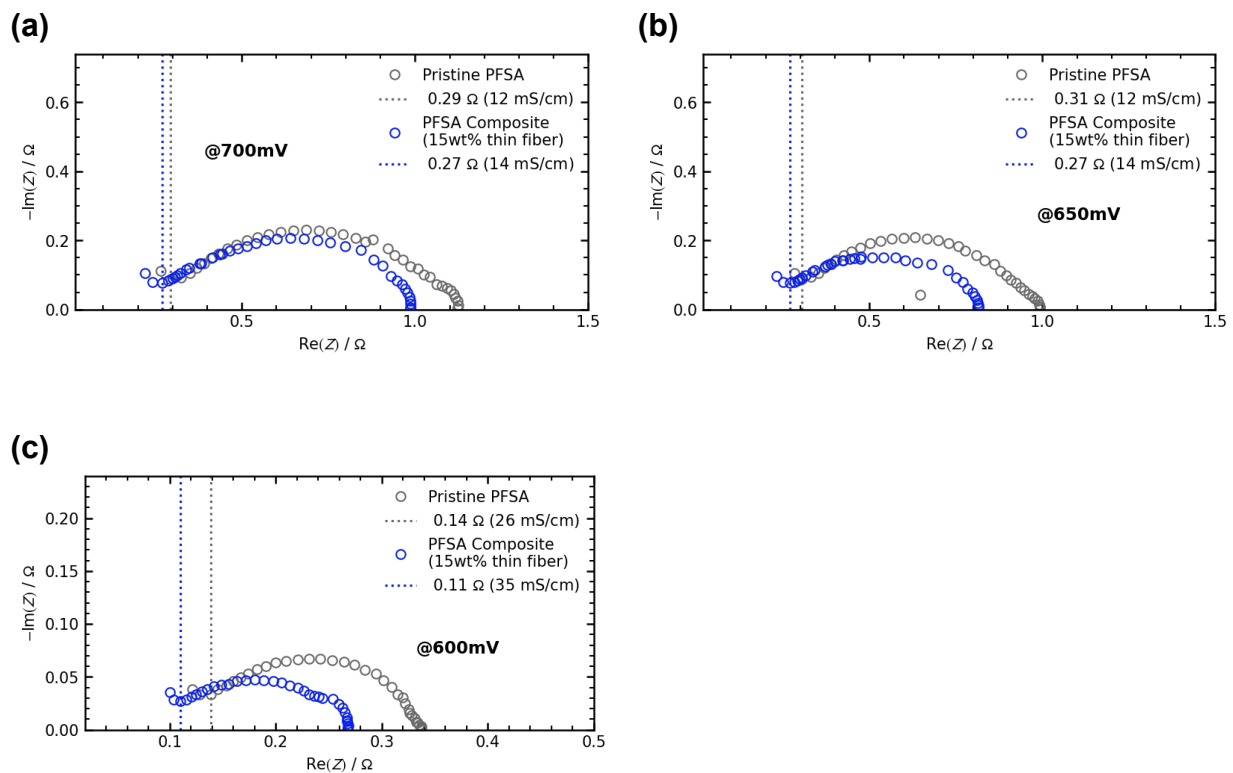
Figure S13. Nyquist plots of the FCs operated in (a) 0.7 V, (b) 0.65 V, and (c) 0.6 V at 120°C (24% RH@anode and 19% RH@cathode). The dotted lines show R_{ohm}.

REFERENCES

1. Li, D.; Takarada, W.; Ashizawa, M.; Yamamoto, T.; Matsumoto, H. Effect of Hydrogen–Deuterium Exchange in Amide Linkages on Properties of Electrospun Polyamide Nanofibers. *Polymer* **2021**, *229*, 123994. DOI: 10.1016/j.polymer.2021.123994.

2. de Almeida; S. H., Kawano, Y. Thermal Behavior of Nafion Membranes. *J. Therm. Anal. Calorim.* **1999**, *58*, 569–597. DOI: 10.1023/A:1010196226309

3. Suzuki, K.; Tanaka, M.; Kuramochi, M.; Yamanouchi, S.; Miyaguchi, N.; Kawakami, H. Development of Blend Nanofiber Composite Polymer Electrolyte Membranes with Dual Proton Conductive Mechanism and High Stability for Next-Generation Fuel Cells. *ACS Appl. Polym. Mater.* **2023** *5*, 5177–5188, DOI: 10.1021/acsapm.3c00656

4. Guan, P.; Zou, Y.; Zhang, M.; Zhong, W.; Xu, J.; Lei, J.; Ding, H.; Feng, W.; Liu, F.; Zhang, Y. High-Temperature Low-Humidity Proton Exchange Membrane with "Stream-Reservoir" Ionic Channels for High-Power-Density Fuel Cells. *Sci. Adv.* **2023**, *9*, eadh1386. DOI: 10.1126/sciadv.adh1386

5. Simari, C.; Lufrano, E.; Brunetti, A.; Barbieri, G.; Nicotera, I. Polysulfone and Organo-Modified Gaphene Oide for New Hybrid Proton Exchange Membranes: A Green Alternative for High-Efficiency PEMFCs. *Electrochim. Acta* **2021**, *380*, 138214. DOI: 10.1016/j.electacta.2021.138214

6. Ballengee, J. B.; Haugen, G. M.; Hamrock, S. J.; Pintauro, P. N. Properties and Fuel Cell Performance of a Nanofiber Composite Membrane with 660 Equivalent Weight Perfluorosulfonic Acid. *J. Electrochem. Soc.* **2013**, *160*, F429. DOI: 10.1149/2.088304jes

7. Breitwieser, M.; Klose, C.; Klingele, M.; Hartmann, A.; Erben, J.; Cho H.; Kerres J.; Zengerle, R.; Thiele, S. Simple fabrication of 12 μm thin nanocomposite fuel cell membranes by direct

electrospinning and printing. *J. Power Sources* **2017**, *337*, 137–144. DOI: 10.1016/j.jpowsour.2016.10.094

8. Lee, C.; Na, H.; Jeon, Y.; Hwang, H. J.; Kim, H.-J.; Isao Mochida, I.; Yoon, S,-H.; Park, J.-I.; Shul, Y.-G. Poly(ether imide) Nanofibrous Web Composite Membrane with SiO$_2$/Heteropolyacid Ionomer for Durable and High-Temperature Polymer Electrolyte Membrane (PEM) Fuel Cells. *J. Ind. Eng. Chem.* **2019**, *74*, 7–13. DOI: 10.1016/j.jiec.2019.01.034

9. Aricò, A. S.; Di Blasi, A.; Brunaccini, G.; Sergi, F.; Dispenza, G.; Andaloro, L.; Ferraro, M.; Antonucci, V.; Asher, P.; Buche, S.; Fongalland, D.; Hards, G. A.; Sharman, J. D. B.; Bayer, A.; Heinz, G.; Zandonà, N.; Zuber, R.; Gebert, M.; Corasaniti, M.; Ghielmi, A.; Jones, D. J. High Temperature Operation of a Solid Polymer Electrolyte Fuel Cell Stack Based on a New Ionomer Membrane. *Fuel Cells* **2010**, *10*, 1013–1023. DOI: 10.1002/fuce.201000031